Electronic Supplementary Material (ESI) for ChemComm.

Sensitized photon upconversion in anthracene-based metal-organic frameworks

J. M. Rowe, J. Zhu, E. M. Soderstrom, Wenqian Xu, Andrey Yakovenko, and A. J. Morris[a]
[a]Department of Chemistry, Virginia Tech, Blacksburg, Virginia 24061, United States

Table of contents

Section 1. MOF synthesis and characterization……..……2
Materials……..……2
Synthesis of 9,10-MOF……..……..……2
Scanning electron microscopy (SEM) ……..……..……..……2
Powder X-ray diffraction (PXRD) ……..……..……3
Gas sorption isotherms……..……..……..……3
Thermogravimetric analysis (TGA) ……..……..……3

Section 2. Structure determination and refinement of 9,10-MOF…….……4
Calculation of structure factor phases……..……..…..……6
Generation and visualization of envelope densities……...……..……6

Section 3. Spectroscopic measurements
Steady-state absorption spectroscopy……..……...……10
Steady-state emission spectroscopy and time-resolved emission lifetimes……...……10
Sample preparation for UC measurements ……...……...……..…11
Upconversion measurements…….……...……..……11

Section 1. MOF synthesis and characterization

Materials. 9,10-anthracenedicarboxylic acid (9,10-ADCA) 2,6-anthracenedicarboxylic acid (2,6-ADCA) and 1,4-anthracenedicarboxylic acid (1,4-ADCA) were used from a prior study.[1] The 2,6-MOF and 1,4-MOF were synthesized according to previously described methods.[2] The 9,10-MOF was prepared by following a literature procedure.[3] Meso-porphyrin IX (MP) was obtained from frontier scientific. Dimethylformamide was purchased from Alfa-Aeser and used as received. To prepare Pd(II) mesoporphyrin IX (PdMP), MP (0.12 mmol) and K_2PdCl_4 (0.24 mmol) were added to DMF (4 mL) and the solution was refluxed overnight. The product precipitated upon the addition of DI water then collected by filtration and dried under vacuum. To anchor PdMP to the surface of 9,10-MOF, 5 mg of MOF were added to a 1.5 mM solution of PdMP in DMF and heated at 45 ºC for 3 hours then soaked at RT overnight. Excess PdMP was removed by washing with DMF and the surface-modified 9,10-MOFs were collected via centrifugation. All other chemicals and solvents including, ZrCl4, N,N′-dimethylformamide (DMF, HPLC grade > 99%), acetic acid (reagent grade > 99%), and formic acid (reagent grade > 99%) were used as received without further purification from Alfa Aesar, Fisher Scientific, or Sigma-Aldrich.

Synthesis of 9,10-MOF. The 9,10-MOFs were synthesized using the procedures previously described for UiO-66 and UiO-66(An) with some modifications.[1, 2] $ZrCl_4$ (23.3 mg, 0.1 mmol) and 9,10-ADCA (26.6 mg, 0.1 mmol) were added to a 3-dram vial along with DMF (3 mL) and acetic acid (0.6 mL, 120 equivalents). The vial was capped and sealed with Teflon tape and the mixture was ultrasonicated for 15 minutes. The vial was then placed in an oven and heated at 120 ºC for 24 hours. The reaction solution was filtered immediately collect and a light-yellow powder was collected via vacuum filtration then washed with DMF and ethanol and dried in air.

Scanning electron microscopy (SEM). SEM images were collected with a Leo/Zeiss 1550 Schottky field-emission scanning electron microscope equipped with an in-lens detector, operating at 5 kV. Le Bail refinement of the 2,6-MOF powder pattern was performed using Rietica for Windows v2.1 software.

Powder X-ray diffraction (PXRD). PXRD patterns of MOF samples were obtained using a Rigaku Miniflex 600 with Cu(Kα) radiation (Cu−Kα = 1.5418 Å) in continuous scanning mode (10.0°/min) and a resolution of 0.1° 2θ.

Gas sorption isotherms. N_2 sorption isotherm measurements were collected on a Quantachrome Autosorb-1 at 77 K. The samples were placed in a 9 mm large bulb sample cell, which was degassed under vacuum for 24 h at 120 °C. The surface areas of the materials were determined by fitting the adsorption data within the 0.05-0.25 P/P_0 pressure range to the BET equations.

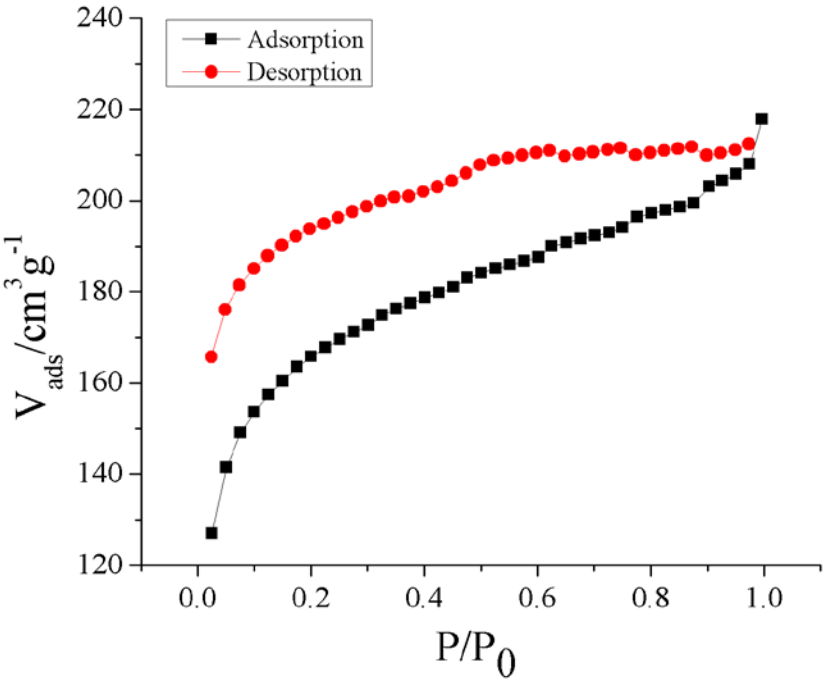

Fig. S1. N_2 sorption isotherm of 9,10-MOF

Thermogravimetric analysis (TGA). TGA data was collected using a Q-series TGA from TA instruments to analyze thermal stability of materials. 10 mg of sample in a high temperature platinum pan were heated under N_2 from 25 °C to 800 °C at a heating rate of 10 °C/min.

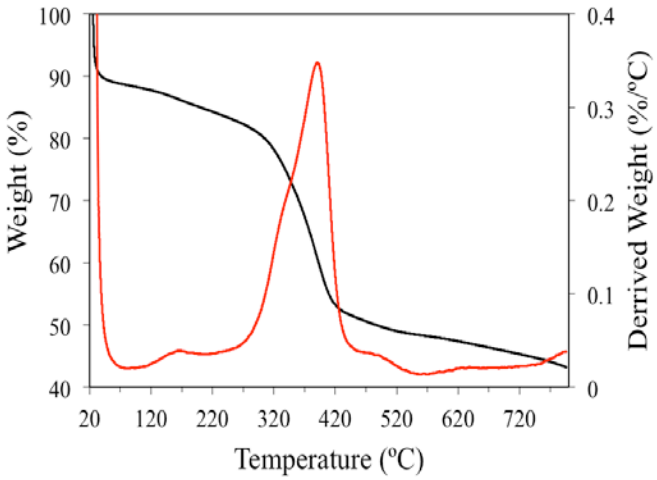

Fig. S2. TGA profile of 9,10-MOF

References

1. J. M. Rowe, J. M. Hay, W. A. Maza, R. C. Chapleski, E. M. Soderstrom, D. Troya, A. J. Morris. J Photochem Photobiol A. 2017, 337, 207.
2. J. M. Rowe, E. M. Soderstrom, J. Zhu, P. M. Usov and A. J. Morris. Can J Chem. 2017.
3. S. Pu, L. Xu, L. Sun and H. Du. Inorg Chem Comm. 2015, 52, 50.
4. M. J. Katz, Z. J. Brown, Y. L. Colon, P. W. Siu, K. A. Scheidt, R. Q. Snurr, J. T. Hupp and O. K. Farha. *Chem. Comm.* 2013. 49.

Section 2. Structure determination and refinement of 9,10-MOF

Synchrotron X-ray powder diffraction of the 9,10-MOF was measured on Beamline 17-BM at Advanced Photon Source (APS), Argonne National Laboratory (in Argonne, IL, USA). The beamline operates in transmission geometry, and is equipped with a PerkinElmer® amorphous silicon area detector that collects two-dimensional diffraction images thru program QXRD [1]. The image data of the 9,10-MOF was integrated with program GSAS-II to an XRD profile of the intensity versus 2-theta format [2]. Indexing of the XRD profile and further refinement analysis was performed with TOPAS version 5. The X-ray wavelength was 0.45260 Å.

Indexing results suggested a face-centered cubic lattice with a lattice constant of 20.9073(1) Å and five candidate space groups, F23, Fm-3, F432, F-43m and Fm-3m. The XRD of 9,10-MOF is similar to that of the well-known UiO-66, which has a space group of Fm-3m and an edge length of 20.7004 Å [3]. From the chemistry point of view, 9,10-Anthracenedicarboxylate in the 9,10-

MOF and benzene-1,4-dicarboxylate in UiO-66 are both bidentate and have the same symmetry. Based on the similarities in both the XRD and the chemical components, the 9,10-MOF is very likely to be isostructural with the UiO-66. An initial structure model of the 9,10-MOF was built based on UiO-66 with the correct ligand. Pawley refinement confirmed the lattice and the space group (Fig. S1 and Table S1). The initial Rietveld refinement showed a poor fit of this framework-only model to the data, as the synthesized sample contained solvent molecules, most likely DMF and water. Adding free oxygen atoms and DMF molecules in the pore improved the fit, but not to level of goodness satisfactory for publishing the refinement. This is due to the inadequacy of approaching the disordered solvent electron density with oxygen atoms or molecular moieties. Hence instead the Difference Envelope Density (DED) ρ_{Δ} method was applied to illustrate the solvent distribution and to further confirm the framework structure.

The DED method has been used very successfully for estimation of MOF guest molecules positions and differences in the framework structures [4-6]. It requires only a few reflection intensities from a PXRD pattern for input. In this application of studying the 9,10-MOF, 10 low angle reflection integrated intensities (F_{obs}^2) were extracted the previous Pawley refinement and used for generation of Structure Envelope (SE) Densities.

Table S1. Final *R*-factors and main refinement parameters of the Pawley whole pattern decompositions.

Compound	**9,10-MOF**
Crystal system	Cubic
Space group	*F m -3 m*
a [Å]	20.9073(1)
d_{min} [Å]	0.96
R_{p} [%]	1.24
R_{wp} [%]	1.65
GOF	1.37

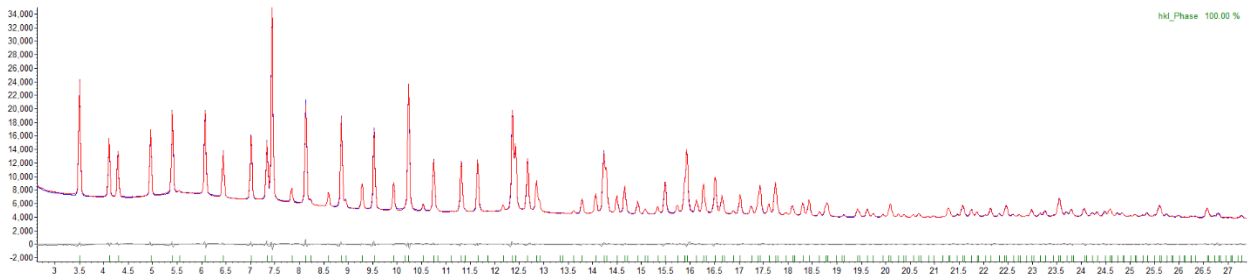

Fig. S3. Pawley refinement plots of the 9,10-MOF XRD data: the whole pattern (top) and an enlarged view of region excluding the two strong low angle peaks (bottom).

Calculation of Structure Factor Phases. The initial model of the 9,10-MOF was used to generate the structure factor phases. In case of the UiO-66, the structural model was taken from a previous publication with the unit cell changed to match that of the 9,10-MOF, a = 20.9073 Å [3]. The ideal intensities F_{calc}^2 for these structures were calculated with XFOG program from SHELXTL software package [7]. Using these intensities the structure factor phases φ_{hkl}^{calc} for the reflections were generated with LIST 2 instruction in the INS-file *via* SHELXL software.

Generation and Visualization of Envelope Densities. Reflections {111}, {002}, {022}, {311}, {222}, {004}, {331}, {422}, {333} and {044} were chosen for Structure Envelope (SE) densities generation in both cases. Combination of F_{calc}^2 and φ_{hkl}^{calc} were used for generation of the calculated SE densities for the 9,10-MOF and UiO-66 ρ_{calc}, while the combinations of F_{obs}^2 a and φ_{hkl}^{calc} were used to create observed SE density ρ_{obs} for the 9,10-MOF. SE densities was produced by SUPERFLIP software [8] in XPLOR format and visualized with UCSF Chimera software [9] (Fig. S2a and 2b). The contents of input SUPERFLIP files (INFIP-format files) can be found below. Difference Envelope Densities (DED) ρ_{Δ} (Fig. S2c and Fig. S3) was generated similarly as previously described. DED built from ρ_{obs} and ρ_{calc} for the 9,10-MOF (Fig. S2c) contains peaks which are located only in the pores of the framework and correspond to the disordered solvent molecules within the cavities. It is important to mention that we did not observe any peaks located in close proximity to the atomic positions of the framework. This suggests the overall structural model for the framework of the 9,10-MOF is correct. In addition, DED $\rho_{\Delta\text{UiO-66}}$ shows the difference between ρ_{obs} for the 9,10-MOF and ρ_{calc} for the UiO-66 (Fig. S3). Besides similar solvent peaks, this DED map also contains peaks on each side of the benzene ring, which is

attributed to the signal from the two additional rings of the anthracene. This also confirms the presence and layout of the anthracenedicarboxylate ligand in the structure of the 9,10-MOF.

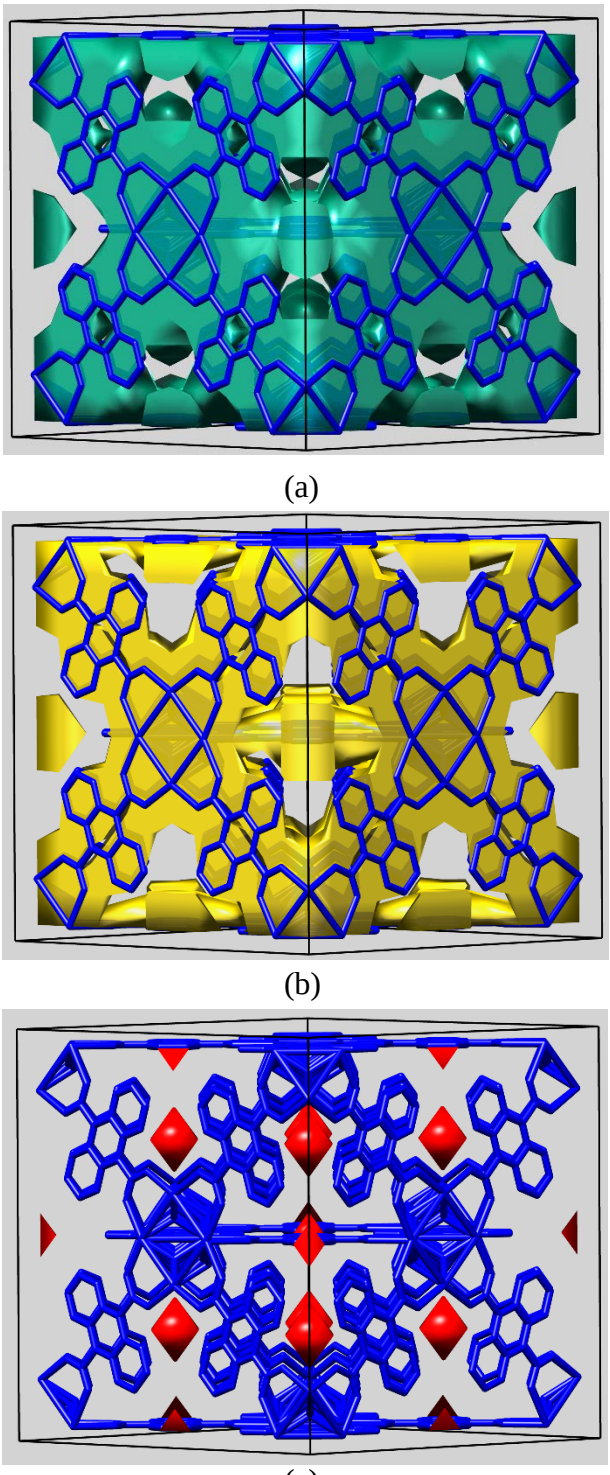

Fig. S4. Structural model of the 9,10-MOF overlapped with Structure Envelopes generated from 9,10-MOF data sets: (a) observed ρ_{obs}, (b) calculated ρ_{calc} and their (c) Difference Envelope Density ρ_{Δ}

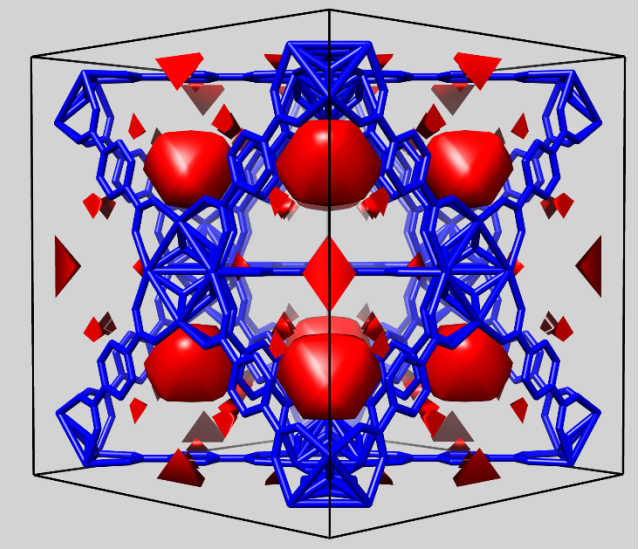

Fig. S5. Structural model of UiO-66 overlapped with Difference Envelope Density $\rho_{\Delta UiO\text{-}66}$ generated as the difference between ρ_{obs} for the 9,10-MOF and ρ_{calc} for the UiO-66

References

1. http://qxrd.sourceforge.net/
2. Toby, B. H., & Von Dreele, R. B. (2013). "GSAS-II: the genesis of a modern open-source all purpose crystallography software package". Journal of Applied Crystallography, 46(2), 544-549.
3. Cavka, J. H.; Jakobsen, S.; Olsbye, U.; Guillou, N.; Lamberti, C.; Bordiga, S.; Lillerud, K. P. J. Am. Chem. Soc. 2008, 130, 13850
4. Chen, Y.-P., Liu, Y., Liu, D., Bosch, M. & Zhou, H.-C. Direct Measurement of Adsorbed Gas Redistribution in Metal–Organic Frameworks. *J. Am. Chem. Soc.* **137,** 2919-2930, (2015).
5. Wriedt, M. *et al.* Low-Energy Selective Capture of Carbon Dioxide by a Pre-designed Elastic Single-Molecule Trap. *Angew. Chem. Int. Ed.* **51,** 9804-9808, (2012).
6. Yakovenko, A. A. *et al.* Study of Guest Molecules in Metal–Organic Frameworks by Powder X-ray Diffraction: Analysis of Difference Envelope Density. *Cryst. Growth Des.* **14,** 5397-5407, (2014).
7. Sheldrick, G. M. *SHELXTL 2008/4 Structure Determination Software Suite*. (Bruker AXS, Madison, Wisconsin, USA, 2008).
8. Palatinus, L. & Chapuis, G. SUPERFLIP - a computer program for the solution of crystal structures by charge flipping in arbitrary dimensions. *J. Appl. Crystallogr.* **40,** 786-790, (2007).
9. Pettersen, E. F. *et al.* UCSF Chimera—A visualization system for exploratory research and analysis. *J. Comput. Chem.* **25,** 1605-1612, (2004).

Section 3. Spectroscopic measurements

Steady-state absorption spectroscopy. The steady-state absorption spectra were obtained using an Agilent Technologies 8453 UV-Vis diode array spectrophotometer (1 nm resolution) where the spectra were recorded with samples prepared in a 1 cm quartz cuvette. The same instrument was used to obtain diffuse reflectance spectra of MOF powders, where the sample compartment was replaced with an integration sphere. The powder samples were diluted by mixing with $BaSO_4$.

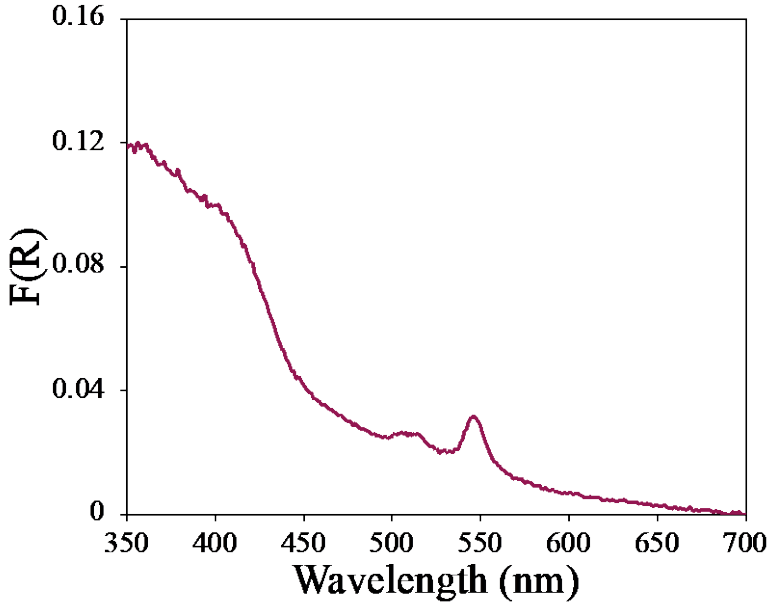

Fig. S6. Diffuse reflectance spectrum of PdMP@9,10-MOF mixed with $BaSO_4$ to dilute.

The concentration of PdMP on the PdMP@9,10-MOF sample was determined by absorption spectroscopy. 475 mg of PdMP@9,10-MOF was dissolved in 1 M NaOH (1 mL), syringe filtered, then diluted with 2 mL of DMF. The molar absorptivity of PdMP at 547 nm in DMF = 30,700 $M^{-1}cm^{-1}$.

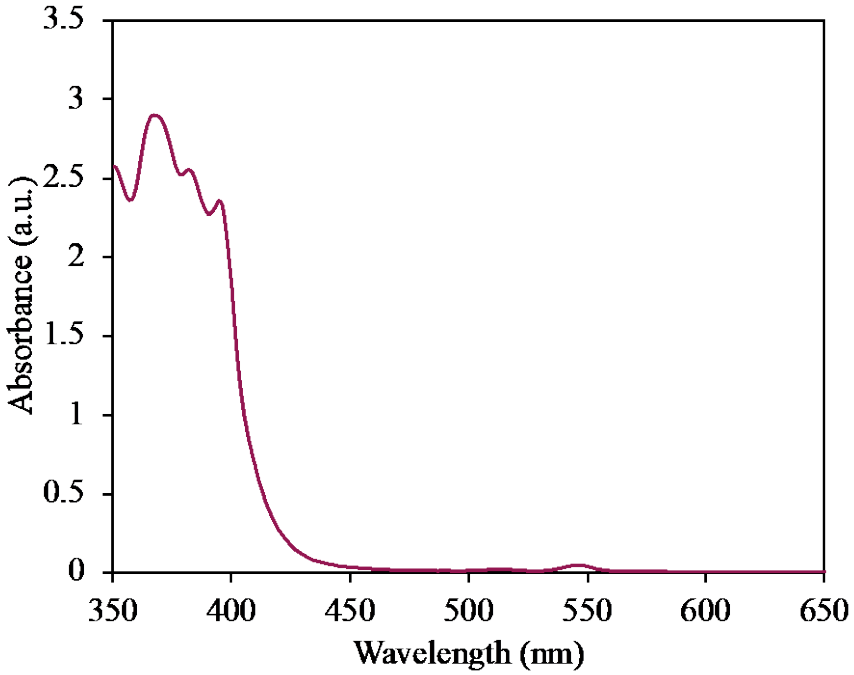

Fig. S7. UV-vis absorption spectrum of PdMP@9,10-MOF after decomposition measured in DMF.

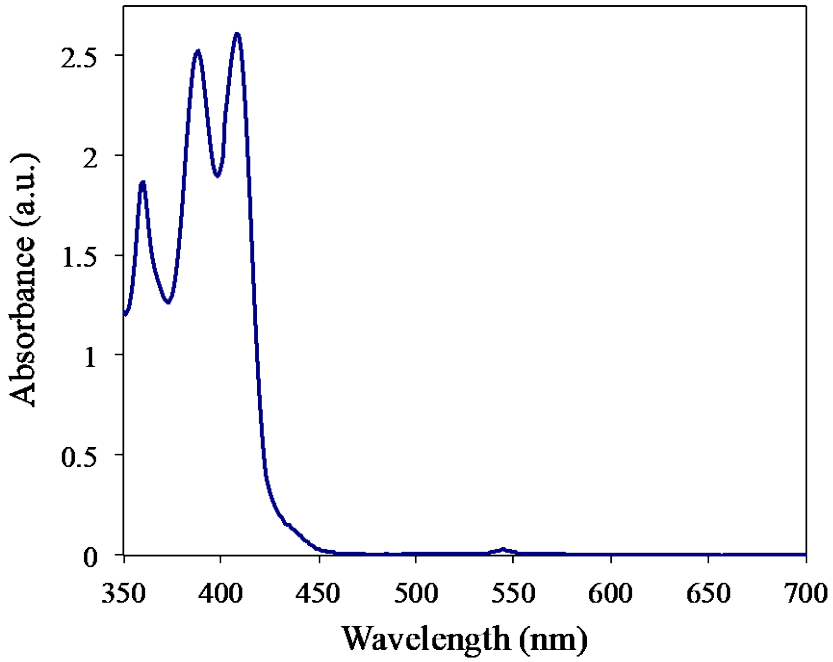

Fig S.8. UV-vis absorption spectrum of PdMP@2,6-MOF after decomposition measured in DMF.

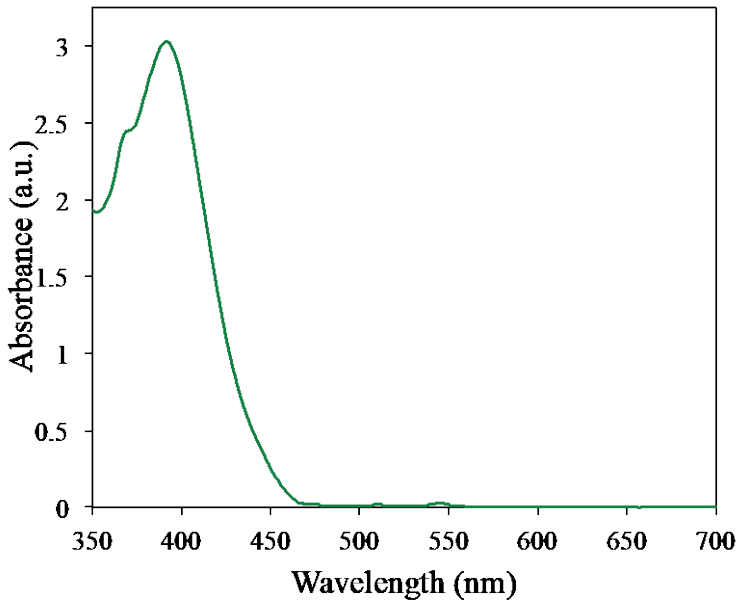

Fig. S9. UV-vis absorption spectrum of PdMP@1,4-MOF after decomposition measured in DMF.

Steady-state emission spectroscopy and time-resolved emission lifetimes. Approximately 3 mg of MOF powder were suspended in 3 mL DMF, all samples were purged with argon before measurements were performed and the sample was continuously stirred during the emission measurements. The ligand samples were prepared at concentrations of ~ 8 μM in DMF. The protonated (ADCA) and deprotonated (ADC^{2-}) ligand samples were prepared in aqueous solutions, using HCl or NaOH to achieve pH values of ~ 2 and 10.5, respectively.

Time-resolved fluorescence lifetime of the 9,10-MOF was obtained via the time-correlated single photon counting technique (TCSPC) with a modified QuantaMaster Model QM-200-4E emission spectrophotometer from Photon Technology, Inc. (PTI) equipped with a 350 nm LED and a Becker & Hickl GmbH PMH-100 PMT detector with time resolution of < 220 ps FWHM. Florescence lifetime decays were deconvoluted from the time-dependent florescence signal and the instrument response function using the fluorescence decay analysis software, DecayFit, available online (Fluortools, www.fluortools.com, Figures S4-S6). For power dependence studies, the excitation source was replaced by a 532 nm continues wave laser and the incident power was tuned using neutral density filters.

Quantum yields of fluorescence and steady-state emission spectra were measured in DMF. The steady-state emission spectra were obtained using the same QuantaMaster Model QM-200-

4E where the sample compartment was replaced with an integrating sphere (PTI). The excitation light source was a 75 W Xe arc lamp (Newport). The detector was a thermoelectrically cooled Hamamatsu 1527 photomultiplier tube (PMT). Measurements were performed in triplicate using three separately prepared suspensions of MOF. Kinetic traces were analyzed using Origin.

To ensure stability of the MOF and the absence of free linker, the solutions were syringe filtered and emission was monitored at the maximum wavelength of emission for each ligand after the emission experiments were completed.

Sample preparation for UC measurements. Sample solutions of 0.35 mM ADCA ligand and 43 μM PdMP were prepared in DMF and deaerated by purging with Ar for ~ 30 minutes. The MOF powders were suspended in DMF and the samples were deaerated by purging with Ar for ~ 1 hour.

Upconversion measurements. Single wavelength emission decay kinetics spectra were recorded using an LP 920 laser flash photolysis system (Edinburgh Instruments) equipped with a PMT detector (R928, Hamamatsu), using either a 355 nm or 532 nm Nd:YAG laser (Spectra-Physics Quanta-Ray Lab) operating at 1 Hz as the excitation source. This same laser system, equipped with an image intensified CCD (ICCD) camera detector, was used to collect time-gated emission spectra. The upconversion quantum efficiencies (Φ_{UC}) and energy transfer efficiencies (Φ_{ET}) were determined from this data by comparing the prompt and delayed fluorescence signals.

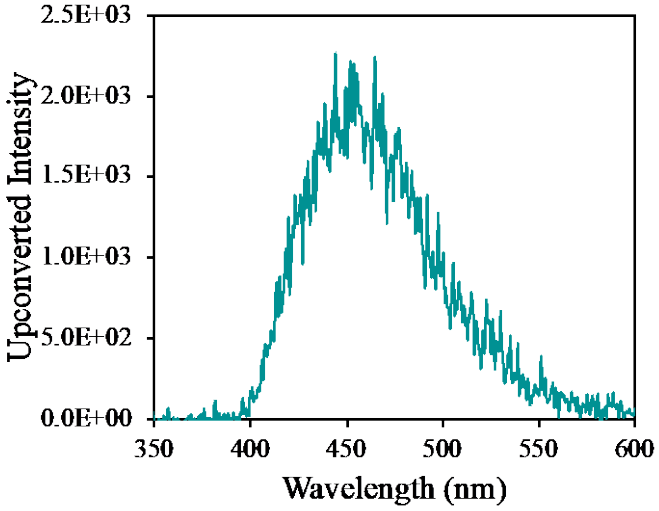

Fig. S10. Emission spectrum for sample of 9,10-ADCA/PdMP sample excited at 532 nm

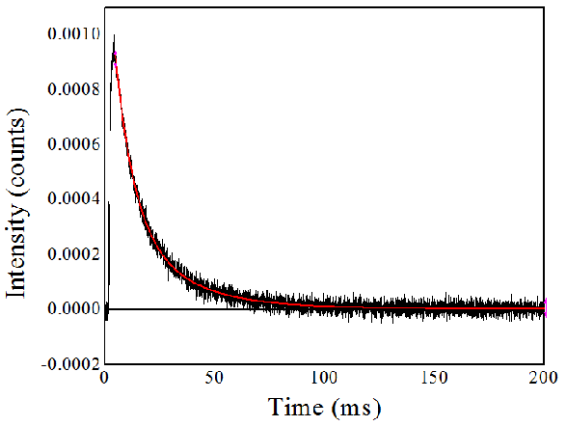

Fig. S11. Emission decay measured at 460 nm excited at 532 nm for sample for 9,10-ADCA/PdMP sample and monoexponential decay fit

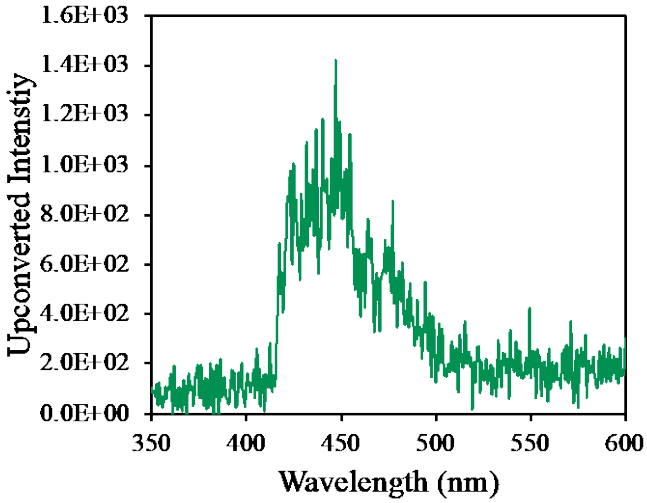

Fig. S12. Emission spectrum for sample of 2,6-ADCA/PdMP sample excited at 532 nm

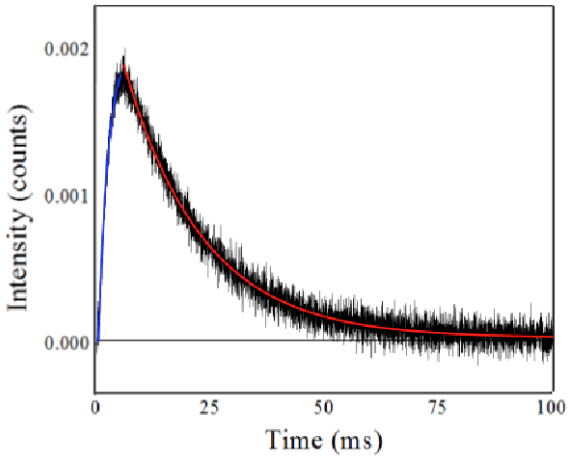

Fig. S13. Emission decay measured at 440 nm excited at 532 nm for sample for 2,6-ADCA/PdMP sample and monoexponential decay fit

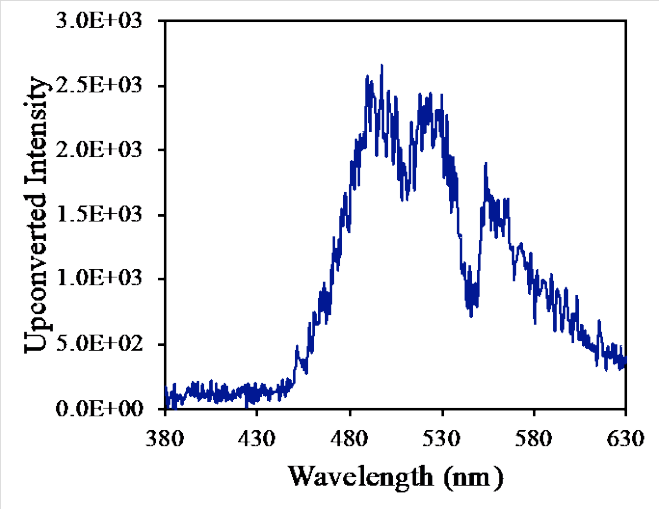

Fig. S14. Emission spectrum for sample of 1,4-ADCA/PdMP sample excited at 532 nm

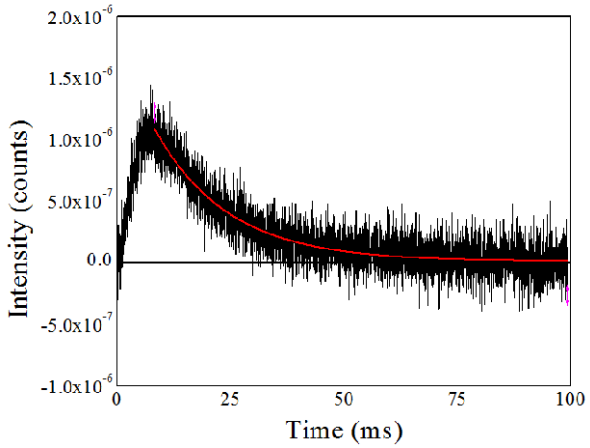

Fig. S15. Emission decay measured at 490 nm excited at 532 nm for sample for 1,4-ADCA/PdMP sample and monoexponential decay fit

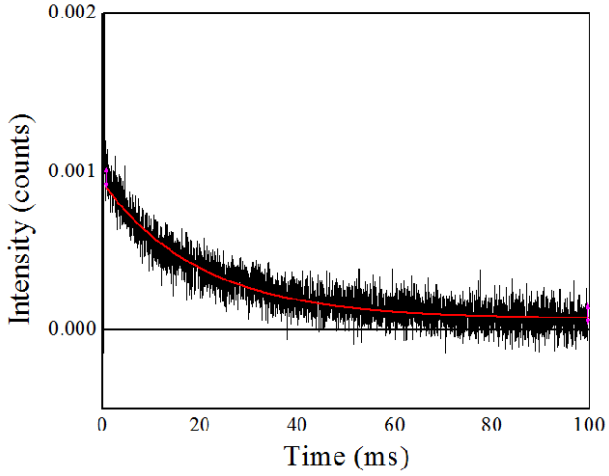

Fig. S16. Emission decay measured at 666 nm excited at 532 nm for sample for PdMP in DMF and monoexponential decay fit

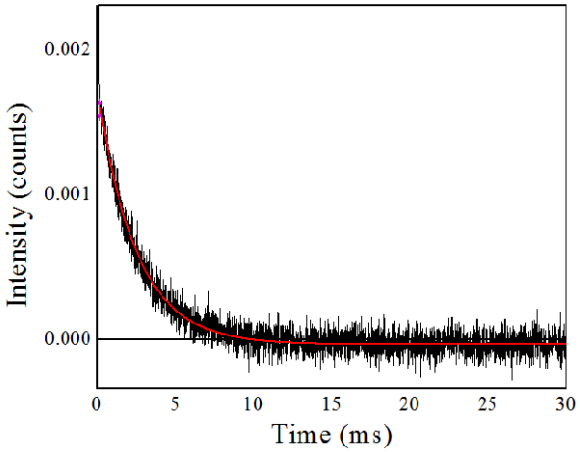

Fig. S17. Emission decay measured at 666 nm excited at 532 nm for sample for 9,10-ADCA/PdMP sample and monoexponential decay fit

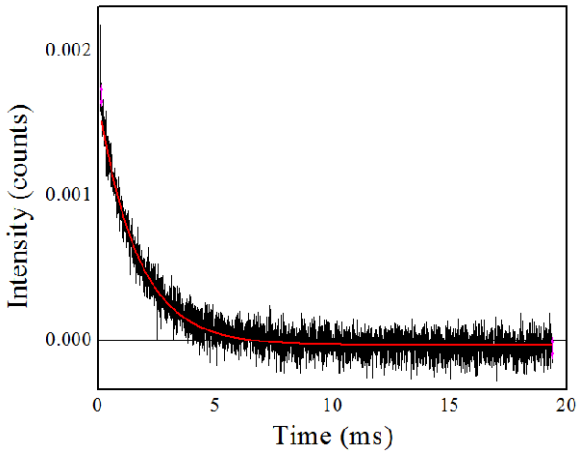

Fig. S18. Emission decay measured at 666 nm excited at 532 nm for sample for 2,6-ADCA/PdMP sample and monoexponential decay fit

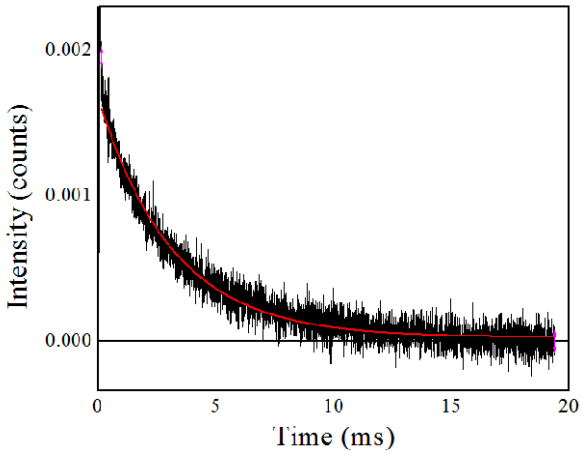

Fig. S19. Emission decay measured at 666 nm excited at 532 nm for sample for 1,4-ADCA/PdMP sample and monoexponential decay fit

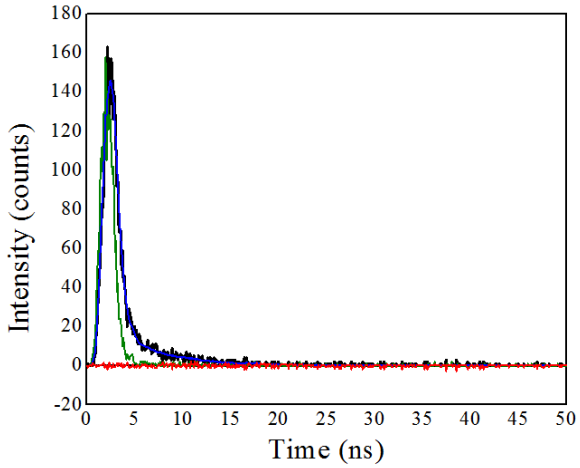

Fig. S20. Raw data from TCSPC measurement of 9,10-MOF emission at 370 nm using 310 nm excitation (black circles), including the instrument response function (red line) and lifetime decay fit (blue line).

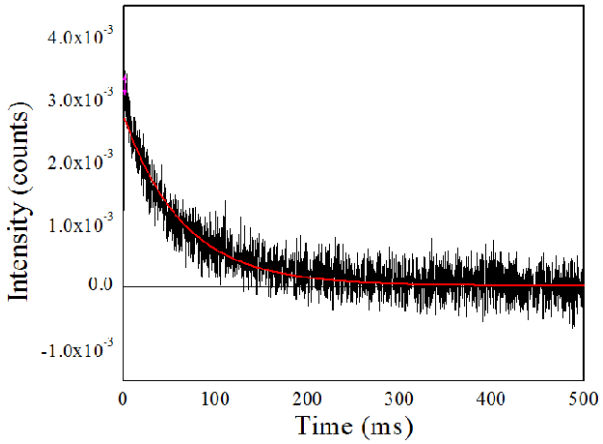

Fig. S21. PdMP@9,10-MOF emission kinetics measured at 470 nm under 532 nm excitation.

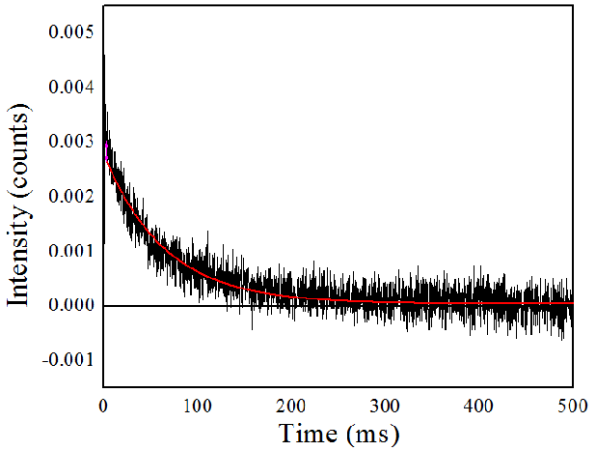

Fig. S22. PdMP@9,10-MOF emission kinetics measured at 666 nm under 532 nm excitation.